



*Minimizing risk. Maximizing potential.®*

# Risk-Based Approach – Explosions and Blast Loading

## Introduction to Explosions and Structure Blast Loading Phenomena

An ioMosaic White Paper

[Marcel Amorós](#)

[Neil Prophet](#)

### Abstract

The major concerns for anyone involved with risk assessment related to explosions is to estimate the explosion wave shape and the overpressure and impulse as a function of distance from the explosion. This paper introduces the fundamentals of explosions and reviews different types of explosions; i.e., physical explosions, vapor cloud explosions, condensed phase explosions, confined explosions with reactions and dust explosions. Additionally, this paper is focused on blast loading phenomena to structures, which is a key input to consider when performing structural response predictions by using the Single Degree of Freedom (SDOF) approach.



## Table of Contents

<b>I. Abstract</b> .....	<b>i</b>
<b>II. Introduction to Explosions</b> .....	<b>1</b>
A. Physical Explosions .....	1
B. Vapor Cloud Explosions.....	3
C. Condensed Phase Explosions .....	4
D. Confined Explosions with Reactions .....	5
E. Dust Explosions .....	5
<b>III. Deflagrations and Detonations</b> .....	<b>6</b>
<b>IV. Blast Loading on Structures</b> .....	<b>9</b>
A. Blast Wave and Structure Interaction.....	10
B. Blast Loading on Closed Rectangular Structures .....	16
1. Average Front Wall Overpressure, $P_{front}$ .....	16
2. Average Back Wall Overpressure, $P_{back}$ .....	18
3. Average Net Horizontal Overpressure, $P_{net}$ .....	20
4. Roof Overpressure, $P_{roof}$ .....	20
5. Average Side Overpressure, $P_{side}$ .....	26
<b>V. Conclusions</b> .....	<b>27</b>
<b>VI. References</b> .....	<b>28</b>



## List of Tables

Table 01: Blast Phenomena Parameters.....	6
Table 02: Additional Blast Phenomena Parameters .....	13

## List of Figures

Figure 01: Schematic Illustration of a Pressure Wave [12] .....	7
Figure 02: Schematic Illustration of a Shock Wave [12].....	7
Figure 03: Time-Displacement Factor Convention.....	9
Figure 04: Structure Located in Region of Mach Reflection.....	10
Figure 05: Scheme of Blast Wave Interaction with a Rectangular Structure .....	12
Figure 06: Reflected Overpressure Ratio versus Angle of Incidence.....	14
Figure 07: <i>P<sub>front</sub></i> versus Time. Time to Rise <i>tr</i> is Negligible .....	17
Figure 08: <i>P<sub>back</sub></i> versus time.....	19
Figure 09: Net Horizontal Overpressure <i>P<sub>net</sub></i> versus Time.....	20
Figure 10: Areas on Roof and Sides Most Affected by Vortex Action .....	21
Figure 11: Location of Loading Zones on Roof and Sides of Structure .....	21
Figure 12: Local Roof or Side Wall Overpressure Ratio versus Time – Zone 1 .....	22
Figure 13: Local Roof or Side Wall Overpressure Ratio versus Time – Zone 2 .....	22
Figure 14: Local Roof or Side Wall Overpressure Ratio versus Time – Zone 3 .....	23
Figure 15: <i>P<sub>roof</sub></i> or <i>P<sub>side</sub></i> versus Time .....	25



## Introduction to Explosions

An explosion is a sudden and violent release of energy. The violence of the explosion depends on the rate at which energy is released. There are several kinds of energy which may be released in an explosion. Three basic types are: (1) Physical Energy, which may take such forms as pressure energy in gases, strain energy in metals or electrical energy; (2) Chemical Energy; which derives from a chemical reaction; and (3) Nuclear Energy, which is out of the scope of the Chemical Process Industry (CPI). Explosions in the process industry can be classified as follows:

- Physical Explosions; e.g., Boiling Liquid Expanding Vapor Explosions (BLEVEs), Rapid Phase Transition Explosions (RPTs)
- Vapor Cloud Explosions
- Condensed Phase Explosions; e.g., High explosives, Ammonium nitrate, Organic peroxides, Sodium chloride
- Confined Explosions with Reaction (runaway reactions); e.g., Explosion involving vapor combustion, Reactor explosions, other explosions involving liquid phase reactions
- Dust Explosions

### Physical Explosions

A pressure vessel contains stored energy due to its internal pressure and represents an explosion hazard. If the vessel is pressurized beyond its mechanical strength, or the vessel integrity is lost, the energy is released suddenly and significant damage can result. The damage is caused by the pressure wave from the sudden gas release which propagates rapidly outward from the vessel. This pressure wave may be a shock wave, depending on the nature of the failure. Flying fragments from the vessel wall or structure can also cause damage. If the vessel contents are flammable, a subsequent fire or vapor cloud explosion might result [1].

The energy contained in the compressed gas within the vessel is used to (1) stretch and tear the vessels walls, (2) provide kinetic energy to the fragments and (3) provide energy for the pressure wave. Some of the energy of expansion also becomes “waste” thermal energy which is not concentrated enough to cause any thermal damage [1].

If the vessel contains all gas, the energy for the pressure wave is derived from the rapid expansion of the released gas. If the vessel contains a liquid with a pressurized vapor space, then the result is dependent on the liquid temperature. If the vessel contains both gas and liquid



and the liquid is below its normal boiling point temperature, then the pressure energy is derived from the rapid expansion of the vapor space gases—the liquid remains unchanged and drains out. If the vessel contains both gas and liquid and the liquid is stored under pressure at a temperature above its normal boiling point, then the pressure wave may derive additional energy from the rapid flashing of a portion of the liquid [1].

There are four methods used to estimate the energy of explosion for a pressurized gas: Brode's equation, isentropic expansion, isothermal expansion and thermodynamic availability [1]. Detailed information related to physical explosions can be found in references [2], [3], [4], [5] and [6].

### ***BLEVEs***

A BLEVE, or boiling liquid expanding vapor explosion, occurs when a vessel containing liquid above its normal boiling point fails catastrophically. The rapid depressurization during vessel failure results in sudden flashing of part of the liquid into vapor. The damage is caused, in part, by the pressure wave from the rapid flashing of the liquid and expansion of the vapor. Projectile damage from the container pieces and impingement damage from ejected liquids and solids is also possible. Vessel failure can result from an external fire, mechanical impact, corrosion, excessive internal pressure or metallurgical failure [1].

For example, for a given vessel exposed to an external fire, the vessel walls below the liquid level are protected by heat transfer from the wall to the liquid, keeping the wall temperature low and maintaining the wall strength and structural integrity.

However, the vessel walls above the liquid level are not protected due to poor heat transfer between the metal wall and the vapor, resulting in an increase in wall temperature and eventual structural failure due to loss of metal strength. The failure may occur at a vessel pressure well below the rated pressure of the vessel or the set pressure of the relief system. After the vessel fails, the liquid flashes almost instantaneously into vapor, resulting in a pressure wave and a vapor cloud. If the liquid is flammable and is ignited, a large fireball will form. The damage effects for this case include the overpressure from the vessel failure, thermal radiation and possible flame impingement from the fireball. BLEVEs can occur with vessels containing noncombustible liquids such as water. The damage effects for this case are due to the overpressure from the vessel failure, fragments from the vessel and impingement of the escaping hot water [1].

Additional information on BLEVEs can be found in references [3], [7]. Methods are available to estimate BLEVE fireball size, height, duration thermal radiation effects [4], [6].



### ***Rapid Phase Transition***

A rapid phase transition explosion occurs when a liquid or solid undergoes a very rapid change in phase. If the phase change is from liquid to gas, or from solid to gas, the volume of the material will increase hundreds or thousands of times, frequently resulting in an explosion. The most common rapid phase transition explosion is due to the sudden exposure of a material to another material which is at a high enough temperature to cause the phase change. Key factors in rapid phase transition explosions include a large temperature difference, a boiling point for the material changing phase that is much lower than the temperature of the heat source, a large difference in heat capacity and a large area of contact between the material and the heat source. Examples of rapid phase transition explosions are the following: direct contact with hot oil with water in heat due to failures in heat exchangers, LNG releases due to direct contact with the pool soil [1].

### **Vapor Cloud Explosions**

A vapor cloud explosion occurs when a large quantity of flammable vapor or gas is released, mixes with air and is subsequently ignited. The vapor or gas fuel is usually released due to the loss of process containment. This could include the failure of a pipe, storage vessel or a process reactor. The rapid discharge of flammable process material through a relief system may also result in a VCE. The vapor may also originate from liquid stored under-pressure to maintain it in the liquid state; i.e., the discharged liquid will flash rapidly into vapor at ambient pressure. The resulting explosion produces an overpressure which propagates outward from the explosion site as a blast wave. Significant damage from the resulting fireball is also possible due to thermal radiation. Several conditions are generally present for a VCE to result in damaging overpressure [1]:

- The released material must be flammable
- A cloud of sufficient size must form prior to ignition. If the cloud is too small, or is ignited early in the release, only a small fireball will result without significant overpressures. A jet or pool fire may subsequently form
- The vapor cloud must mix with air to produce a sufficient mass in the flammable range of the material released. Without sufficient air mixing, a diffusion controlled fireball may result without significant overpressures developing
- The speed of the flame propagation must accelerate as the vapor cloud burns. Without this acceleration, only a flash fire will result, which may produce significant damage due to thermal radiation and direct flame impingement



Flame acceleration is an important part of the vapor cloud explosion. The flame accelerates when turbulence stretches and tears the flame front increasing its surface area. The primary turbulence sources are flow turbulence established in the unburned gas as it flows ahead of the flame front, pushed by the expanding combustion products behind it; and turbulence caused by the interactions of the gas with obstacles it encounters. In either case the turbulence results from the motion of the gas [1].

As the turbulence increases, stretching the flame front, the rate at which the fuel is combusted increases because the area of the stretched and torn flame front has increased. As the rate of combustion increases the force on the unburned gases increases, causing them to move even faster, increasing the turbulence further. This creates a feedback mechanism that accelerates the flame speed. Turbulence from the release could be a contributing factor near the point of release, but flame front acceleration to damaging overpressures can occur even in initially quiescent gas in a congested or confined process area. A congested process area, populated with pipes, pumps, valves, vessels and other process equipment is adequate to result in significant flame speed acceleration. Most VCEs result in deflagrations and detonations are unlikely. Increasing levels of confinement and congestion increase the explosion overpressure. While vapor cloud detonations are rare, the higher overpressures can approach the severity of detonations [1].

Several methods are available for determining the overpressure-impulse as a function of distance from explosion; e.g., TNT Equivalency, TNO Multi-energy, Baker-Strehlow. Detailed information on explosion modeling can be found in [3], [4], [6], [7] and [8].

## Condensed Phase Explosions

A condensed phase explosion occurs when a solid or liquid material explodes directly from the bulk state. High explosives, such as TNT, are a common example of a condensed phase explosive. There are many solid and liquid materials capable of undergoing very sudden and explosive decomposition or reaction due to exposure to, for example, shock, temperature, pressure and contamination. Examples of these materials include many peroxide and nitrate materials [1].

The equilibrium state for a system is defined as the state with the minimum Gibbs energy. Many chemicals, however, are present at a metastable state. If energy is provided that exceeds the trough or activation energy, then a reaction will occur moving the material to the new equilibrium state. The reaction may occur very suddenly, with the potential release of large volumes of gas or vapor. An explosion may result, with damage due to the blast wave, thermal energy or projectiles [1].



## Confined Explosions with Reactions

Runaway reactions are possible whenever an exothermic reaction is encountered. This can occur within a reactor, storage vessel or even an open pool or container. Several factors have been identified that can lead to runaway reaction. For example, for a loss of coolant accident involving a very exothermic reaction due to insufficient heat removal and high heat release of intended reaction [1]. The details on reaction system dynamics is out of the scope of the present paper and more detailed information can be found in references [6], [9], [10].

## Dust Explosions

Any solid material that can burn in air will do so with a violence and speed that increases with increasing degree of subdivision of the material. The smaller the particle size, the greater the combustion rate because the total contact surface area between the combustible dust and air increases [11]. Potential dust explosions are considered during risk-based quantitative assessments if all the following conditions are present at the same time:

- Combustible dust; i.e., small particles of sizes on the order of 0.1 mm or less
- Dispersion of dust particles; i.e., particles are suspended in a sufficiently large volume of air to give each particle enough space for its unrestricted burning
- Presence of an ignition source
- Confinement of dust cloud
- Oxygen in air

When all these elements are in place, rapid combustion can occur.

Detailed information related to dust explosions can be found in references [6] and [11].





## Deflagrations and Detonations

The damage effects from an explosion depend highly on whether the explosion results from a deflagration or a detonation. The difference depends on whether the reaction front propagates below or above the speed of sound in the unreacted gases. The two types of blast waves are illustrated in **Figure 01** and **Figure 02 [12]** and the blast wave phenomena parameters are defined in **Table 01**.

**Table 01: Blast Phenomena Parameters**

Symbol	Parameter
$P_{so}$	Peak side-on positive overpressure [psi]
$P_{so}^-$	Peak side-on negative overpressure [psi]
$P_o$	Atmospheric pressure [psi]
$P_s(t)$	Positive overpressure function with respect to time [psi]
$P_s^-(t)$	Negative overpressure function with respect to time [psi]
$t_A = t_d$	Time of arrival, or time required for a blast wave to travel from the point the center of the explosion to the given location [ms]
$t_0$	Duration of the positive phase of the incident blast wave [ms]
$t_{0^-}$	Duration of the negative phase of the incident blast wave [ms]
$i_s$	Positive impulse [psi·ms]
$i_s^-$	Negative impulse [psi·ms]

1. *Pressure Wave or Deflagration*: Gradual pressure rise to the peak side-on overpressure followed by gradual pressure decay and a negative phase like that for a shock wave. The pressure wave is subsonic.
2. *Shock Wave or Detonation*: Sudden, almost instantaneous rise in pressure above ambient atmospheric conditions to a peak free field (side-on or incident) overpressure. The peak side-on overpressure gradually returns to ambient with some highly damped pressure oscillations. This results in a negative pressure wave following the positive phase of the blast wave. Shock waves in the near and far fields usually result from condensed phase detonations, or from an extremely energetic vapor cloud explosion. Most vapor cloud deflagrations will give rise to pressure waves in the near field which may propagate as a shock wave, or “shock-up,” in the far field. The shock wave travels faster than the speed of sound.

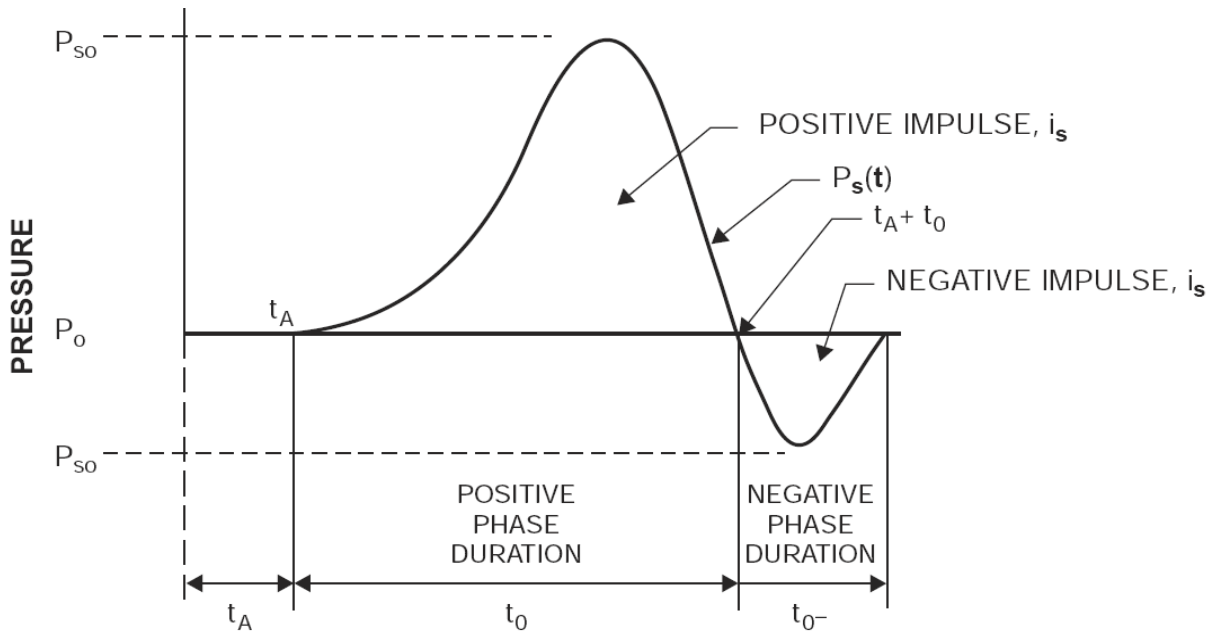


Figure 01: Schematic Illustration of a Pressure Wave [12]

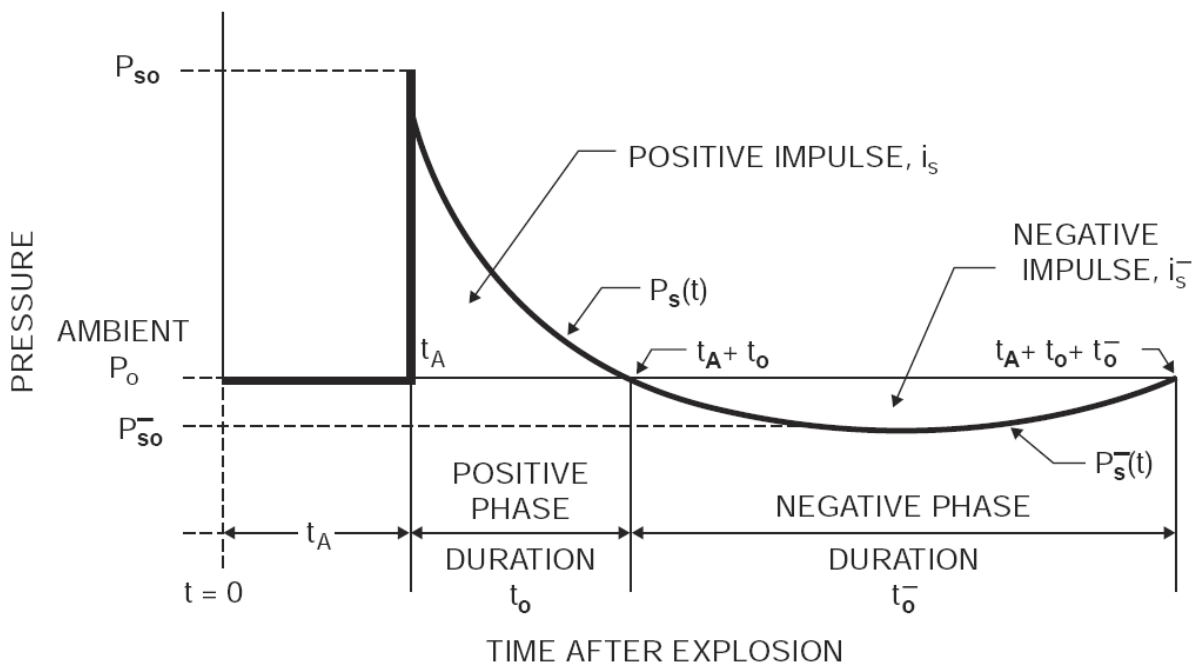


Figure 02: Schematic Illustration of a Shock Wave [12]



The rate of decay of the positive phase varies with respect to the magnitude of the peak overpressure. The peak negative overpressure is approximately one-eighth of the peak positive overpressure and the duration of the negative phase is approximately four times the duration of the positive phase of the blast. The following equation is valid for ideal wave shapes which occur at approximately 10 psi or lower; i.e., most of potential accidental explosions in the Chemical Process Industry (CPI).

For times where  $t_d < t \leq (t_d + t_0)$ , the incident overpressure curve is defined as follows; i.e., positive phase duration:

$$P_s = P_{s0} \left[ 1 - \frac{(t - t_d)}{t_0} \right] e^{-(t-t_d)/t_0} \quad \text{E.01}$$

For times where  $(t_d + t_0) < t \leq (t_d + t_0 + t_0^-)$ , the incident overpressure curve is defined by criteria illustrated in [9], which is based on experimental results and consider  $P_{s0}^-$  as four times less than  $P_{s0}$  and  $t_0^-$  eight times greater than the  $t_0$ .

The major concerns with risk assessment related to explosions are the explosion wave shape and the overpressure and impulse as a function of distance from the explosion. Once these key parameters are known, the damage effects due to people and structures/buildings can be estimated. Detailed damage criteria to humans due to explosions can be found in [13]. No further knowledge is required if the population is outdoors because well-known overpressure thresholds, impulse and probit equations provide the required knowledge for human vulnerability analysis.

However, if more detailed analyses need to be developed for estimating the occupied building human vulnerability and associated building/structure levels of damage, knowledge related to blast loading on structures is needed. Blast loading requires the evaluation of the interaction between the blast wave and the impacted structure and its main purpose is to estimate pressure history profiles at each side/roof of the structure. This information is a critical step before conducting the Single Degree of Freedom (SDOF) approach once the resistance of the structure is known. The development of the SDOF approach can be found in reference [14].



## Blast Loading on Structures

The determination of blast loads on a given structure/building requires knowledge on blast wave phenomena. The key blast wave parameters have been introduced: the magnitude and shape of the blast wave depends on the nature of the energy release and on the distance from the explosion epicenter. Therefore, once defined the incident overpressure and associated impulse, i.e., pressure history profile by using **E.01**, the interaction between the blast wave and the structure can be analyzed. The following contents provide detailed quantitative criteria for blast loading on rectangular structures. The criteria are strictly based on reference **[15]**.

In determining the loads on a structure, it is convenient to use the instant at which the shock front impinges on the front face as a reference for time ( $t = 0$ ). In adopting this convention, it is necessary to introduce a time-displacement factor  $t_d$ , which is the time required for the shock front to travel from the front face of the structure to the surface or point under consideration. **Figure 03** illustrates this convention. In **Figure 03**,  $t - t_d$  is the time after the shock front has passed a given location on the structure and determines the overpressure  $P_s$  in the incident blast wave at that location. For example, the time-displacement factor for a given location on the roof at distance  $L'$  from the front face of the structure is  $t_d = L'/U_0$ , where  $U_0$  is the shock front velocity.

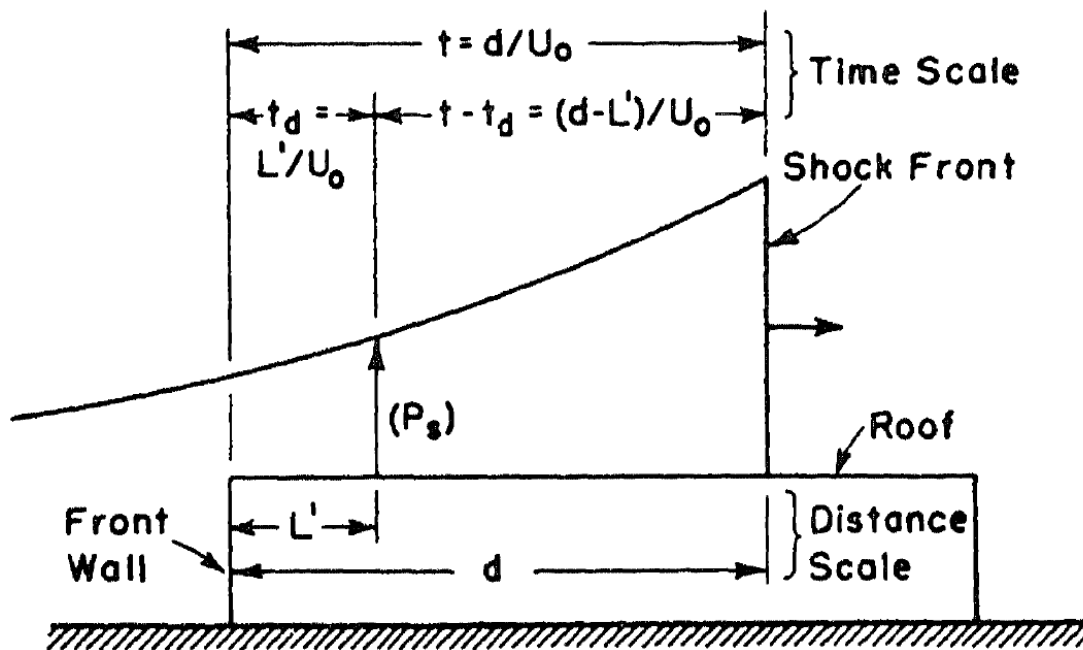


Figure 03: Time-Displacement Factor Convention



For higher overpressure levels, the variation of overpressure with time at the ground level is usually irregular, due to thermal effects and to other modifying influences of the ground surface. Reference [2] contains data on these irregular wave forms. However, due to lack of data and the complexity of calculations involving irregular wave forms, it is recommended to use the ideal wave for practical design purposes. The procedures for the determination of loads are restricted to surface structures located outside the region of regular reflection where the Mach Stem is high enough to cover the structure.

The structure is considered as being oriented with one face normal to the direction of propagation of the shock wave, since such an orientation produces the most severe loading on the structural elements. For the design of a structure so located, it is necessary to predict the overpressures which would exist on various portions of the structure as a function of time measured after the shock front strikes the front wall. The loading on aboveground structures resulting from the air blast produced by an air or surface burst may be considered to consist of a diffraction phase and a drag phase.

1. The *diffraction phase* of the loading is the term given to the initial phase of the blast loading on a structure when the reflected pressures associated with the air blast are acting on the structure. The time required for the blast wave to surround the structure and the presence of large reflected pressures on the front wall resulting in net lateral loads on the entire structure. The local and differential forces which act on the structure during the initial stages are defined as the diffraction phase loading.
2. The *drag phase* of the loading is the term given to the second phase of the loading on a structure due to the mass and velocity of the air particles in the blast wave after the envelopment of the structure by the wave front and the reflection effects have decayed.

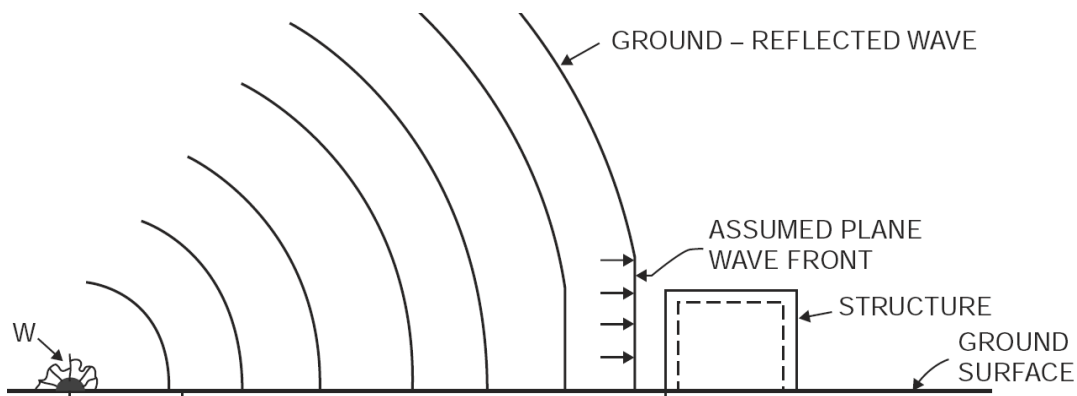


**Figure 04: Structure Located in Region of Mach Reflection**

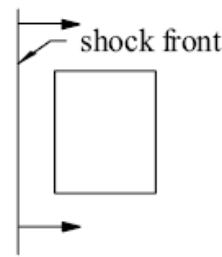
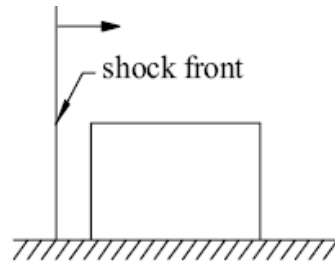


## Blast Wave and Structure Interaction

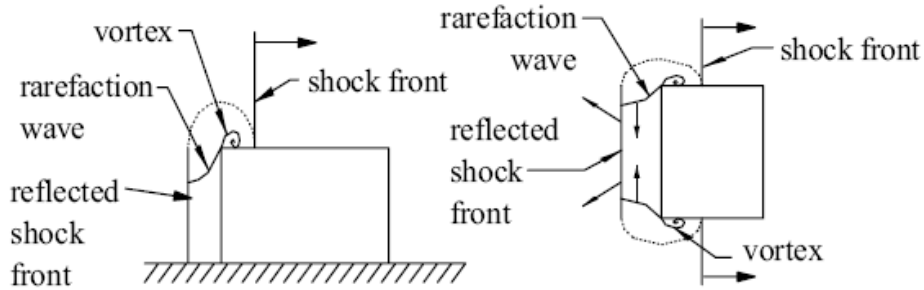
Given the distance from the center of the explosion to the structure/building under analysis and the dimensions of the structure/ building the loads over the entire building can be estimated. The following qualitatively address the blast loading on closed rectangular structures.

The behavior of the blast wave upon striking a closed rectangular structure is depicted in **Figure 05**, which illustrates the position of the shock front and the behavior of the reflected and diffracted waves at successive times during the passage of the blast wave over the center portion of the structure. As the shock front strikes the wall of the building, a reflected blast wave is formed and the overpressure on this wall is raised to a value more than the peak overpressure in the incident blast wave (see **Figure 05a**). This increased overpressure is called the reflected overpressure and is a function of the peak overpressure in the incident blast wave and the angle of incidence of the shock front with the front wall which is zero degree in this case.

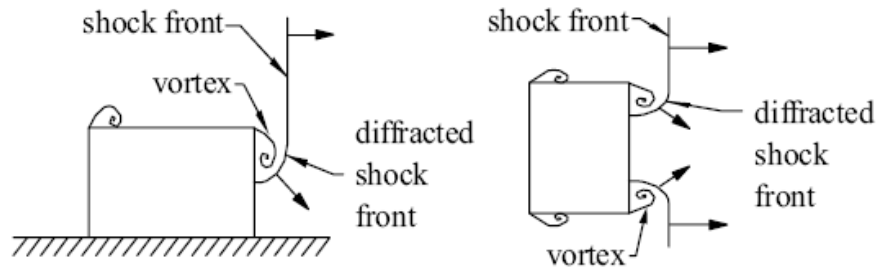
When the reflected shock front is formed, the lower overpressure existing in the incident blast wave adjacent to the top edge of the front wall initiates a rarefaction wave, or a wave of lower overpressure than that which exists in the reflected blast wave (see **Figure 05b**). This rarefaction wave travels with the speed of sound in the reflected blast wave toward the bottom of the front wall. Within a short time, called the clearing time, the rarefaction wave weakens the reflected blast wave to such an extent that its effect is no longer felt and reduces the overpressure existing on the front wall to a value that is in equilibrium with the high-velocity air stream associated with the incident blast wave. When equilibrium with the high-velocity air stream is reached, the overpressure on the front wall is equal to the stagnation overpressure at the base of the front wall with an overpressure somewhat less than that in the blast wave at the top edge of the front wall. The stagnation overpressure is the overpressure existing in a region in which the moving air has stopped, causing the pressure intensity to be increased by the loss in momentum of the air particles.



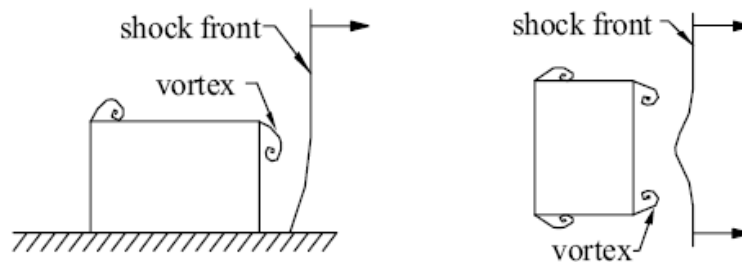
a) Shock front approaches structure



b) Shock reflected from front surface and diffracts over structure



c) Diffraction continues across rear surface



d) Diffraction is complete. Shock front passes beyond structure

**Figure 05: Scheme of Blast Wave Interaction with a Rectangular Structure**



At a time after the shock front strikes the front wall of the structure which is equal to the length of the structure divided by the shock front velocity, the shock front reaches the back edge of the structure and starts spilling down toward the bottom of the back wall (see **Figure 05c**). The back wall begins to experience increased pressures as soon as the shock front has passed beyond it. The effect is first observed at the top portions of the back wall and proceeds toward the bottom.

A vortex, which is a region of air spinning about an axis at a high speed with low overpressures existing at its center, is created on the back wall and grows, traveling toward the base from the top edge and moving away from the wall (see **Figure 05b**). The maximum back wall overpressure develops slowly because of the vortex phenomena and the time required for the back wall to be enveloped by the blast wave. As the shock front passes beyond the front wall (see **Figure 05b**), the overpressure exerted on the roof of the structure is initially raised to a value nearly equal to the overpressure existing in the incident blast wave.

However, the air flow caused by the pressure difference between the reflected overpressure on the front wall and the blast wave overpressure on the roof causes the formation of a vortex along the top edge of the front wall. The vortex travels with a gradually decreasing intensity along the roof of the structure (see **Figure 05c**) at a slower rate than the shock front velocity. It causes a decay of the overpressures built up by the incident blast wave. After the passage of this vortex, the higher overpressures in the blast wave again become dominant and cause a second build-up of overpressures along the roof.

Thus, depending on its distance and orientation relative to the blast source, the building and its components will experience various combinations of blast effects (reflected overpressure, side-on overpressure, dynamic pressure and negative pressure).

In addition to peak overpressure, phase duration and impulse, other blast wave parameters must be evaluated (see **Table 02**).

**Table 02: Additional Blast Phenomena Parameters**

Symbol	Parameter
$P_{r-\alpha}$	Peak Reflected Pressure
$q_o$	Peak Dynamic (blast wind) Pressure
$U_0$	Shock Front Velocity
$L_W$	Blast Wave Length





### Peak Reflected Pressure

When the free field blast wave from an explosion strikes a surface, it is reflected. The effect of this blast wave reflection is that the surface will experience a pressure much more than the incident side-on value. The reflection coefficient depends on the peak overpressure, the angle of incidence of the wave front relative to the reflecting surface and on the type of blast wave.

Reflected overpressure ratio  $P_{r-\alpha}/P_{so}$  is plotted in **Figure 06** as a function of the angle of incidence  $\alpha$  of the shock front. It applies to an inclined shock front striking a reflecting surface such as a wall.

Now, the incident shock front strikes the front wall, the overpressure on the front wall is immediately raised from zero to the reflected overpressure  $P_{refl}$ , in psi, illustrated in Equation **E.02** below:

$$P_{refl} = 2P_{so} \left[ \frac{7 \cdot 14.7 + 4P_{so}}{7 \cdot 14.7 + P_{so}} \right] \tag{E.02}$$

Note that the value of  $P_{refl}$  is the same as  $P_{r-\alpha}$  for  $\alpha = 0^\circ$  using **Figure 05**.

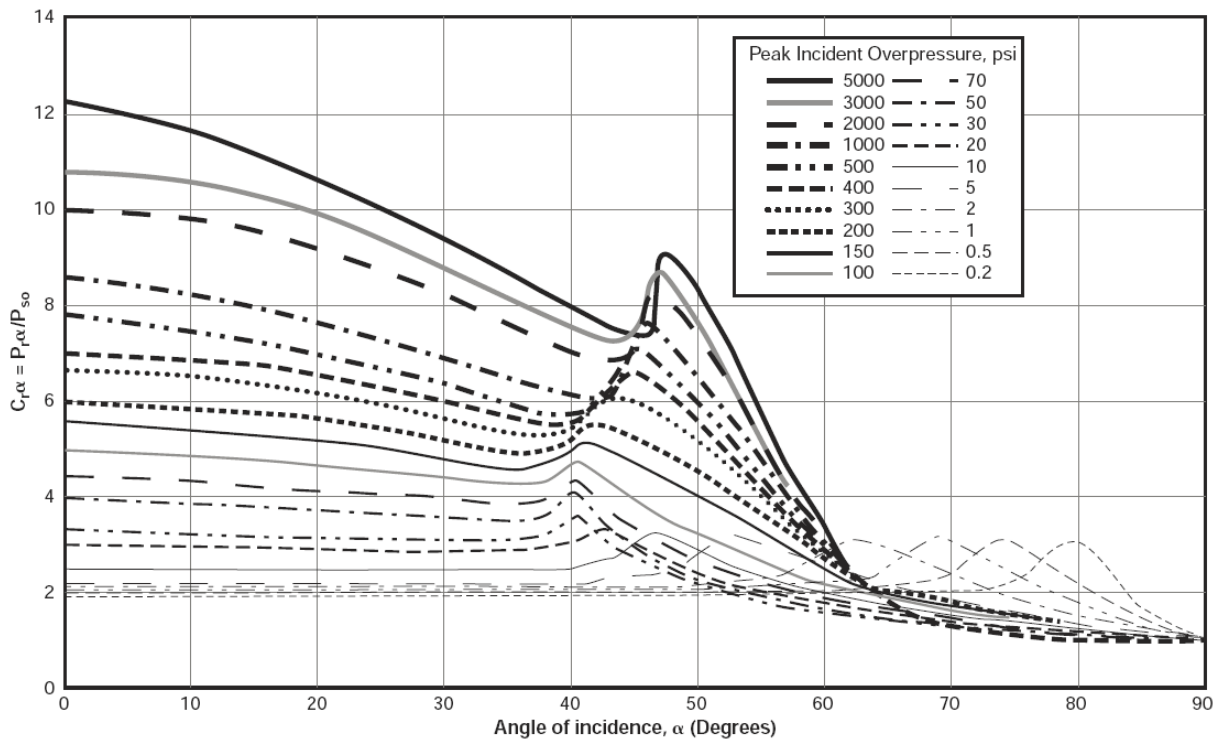


**Figure 06: Reflected Overpressure Ratio versus Angle of Incidence**



The duration of the reflected pressure depends on the dimensions of the reflecting surface, up to a maximum time approximately equal to the positive phase duration of the incident blast wave. This upper limit corresponds to the total reflection of the entire blast wave without any diffraction around the edges of the reflecting surface.

### ***Dynamic Pressure, Blast Wind***

The dynamic pressure or blast wind is a blast effect due to air movement as the blast wave propagates through the atmosphere. The velocity of the air particles and hence the wind pressure, depends on the peak overpressure of the blast wave. The dynamic pressure is defined as follows:

$q$ : Dynamic pressure due to the motion of air particles in the incident blast wave at any time  $(t - t_d)$  and is given by  $q = \rho u^2 / 2$ , where  $\rho$  is the mass per unit volume of the air and  $u$  is the velocity of the air particles. Note that peak dynamic pressure  $q$  for use when overpressures are less than 10 psi is given by Equation **E.03**:

$$q_0 = 14.7 \left[ \frac{\frac{5}{14} \left( \frac{P_{so}}{14.7} \right)^2}{1 + \frac{1}{7} \left( \frac{P_{so}}{14.7} \right)} \right] \quad \text{E.03}$$

To obtain  $q$  as a function of time for overpressures less than 10 psi it is convenient to use the ratio  $q/q_0$  as a function of  $(t - t_d)/t_0$  from the following expression (Equation **E.04**):

$$q = q_0 \left[ 1 - \frac{(t - t_d)}{t_0} \right] e^{-3.5(t-t_d)/t_0} \quad \text{E.04}$$

### ***Shock Front Velocity***

In the free field, the blast wave from an explosion travels at or above the acoustic speed for the propagating medium. The shock front velocity  $U_0$  is a function of the peak overpressure  $P_{so}$ ; and its value for standard atmospheric conditions is plotted for high energy TNT explosives (UFC 3-340-02 [18]). There are no similar plots available for pressure wave propagation. However, for design purposes it can be conservatively assumed that a pressure wave travels at the same velocity as a shock wave. In the low-pressure range and for normal atmospheric conditions, the shock/pressure front velocity in air can be approximated using the following relationship (Equation **E.05**):

$$U_0 = 1117 \sqrt{\left[ 1 + \frac{6P_{so}}{7 \cdot 14.7} \right]} \quad \text{E.05}$$



### **Shock Wave Length**

The propagating blast wave at any instant in time extends over a limited radial distance as the shock/pressure front travels outward from the explosion. The pressure is largest at the front and trails off to ambient over a distance,  $L_w$ , the blast wave length. In the low-pressure range, the length of the blast wave can be approximated by Equation **E.06**:

$$L_w = U_0 t_0 \quad \text{E.06}$$

### **Blast Loading on Closed Rectangular Structures**

#### **Average Front Wall Overpressure, $\bar{P}_{front}$**

Now, the incident shock front strikes the front wall, the overpressure on the front wall is immediately raised from zero to the reflected overpressure,  $P_{refl}$ . The incident shock front continues its motion over the top of the structure, while the reflected shock front moves away from the front of the building in the opposite direction. Initially, the air pressure between the reflected shock front and the front wall is higher than the pressure behind the incident shock front. This causes air to move around to the sides and over the top of the structure into the lower pressure zone behind the incident shock. The rarefaction waves thus formed move from the end and top edges toward the center of the front face with the speed of sound for the pressure existing in this region of reflected overpressure [16].

For the range of shock strengths used in the Princeton shock tube experiments [15] which correspond to peak shock overpressures of 2 to 50 psi in a standard atmosphere, it has been found that the time required to clear the front face of reflection effects is determined by the dimensions of the front face and the peak overpressure of the incident shock wave. This clearing time  $t$  is given by Equation **E.07**:

$$t_c = 3h'/c_{refl} \quad \text{E.07}$$

$h'$ : Clearing height, taken as the full height of the front face or half its length whichever is the smaller

$c_{refl}$ : Velocity of sound in the reflected region, plotted as a function of the peak overpressure of the incident blast wave (Equation **E.08**):

$$c_{refl} = 422 \sqrt{\frac{1.088P_{so}^2 + 70P_{so} + 720}{102.9 + 6P_{so}}} \quad \text{E.08}$$



During the time required to clear the front wall of reflection effects, the average overpressure on the front wall decreases from the reflected overpressure to a value given by Equation E.09:

$$\bar{P}_{front} = P_s + 0.85q \tag{E.09}$$

$P_s$ : Overpressure in the incident blast wave at the front wall at any time  $t - t_d$  as given by Equation E.01:

$q$ : Dynamic pressure due to the motion of air particles in the incident blast wave at any time  $(t - t_d)$  and is given by  $q = \rho u^2 / 2$ , where  $\rho$  is the mass per unit volume of the air and  $u$  is the velocity of the air particles.

\*Note that peak dynamic pressure  $q$  when overpressures are less than 10 psi is given by Equation E.03 and to obtain  $q$  as a function of time, Equation E.04 is applicable.

For the front wall overpressures,  $t_d = 0$  and hence  $(t - t_d) = t$ , where  $t$  measures the time after the instant at which the shock front impinges on the front wall. Using the above quantities, the curve of the average front wall overpressure  $\bar{P}_{front}$  versus time is determined as follows for two different cases: time to rise  $t_r$  is negligible (see Figure 07, left side) and time to rise  $t_r$  is not negligible (see Figure 07, right side).

In Figure 07 (left side), the curve a-b-c is defined by Equation E.09. Point d, the reflected overpressure, is connected by a straight line to point b, the average overpressure at time  $(t - t_d) = t_c$ . Since the resulting discontinuity at point b is not compatible with actual behavior of the loads on the front face, these two curves are smoothed by fairing in curve e-f as shown.

The curve of average overpressure versus time on the front wall is then defined as curve O-d-e-f-c.

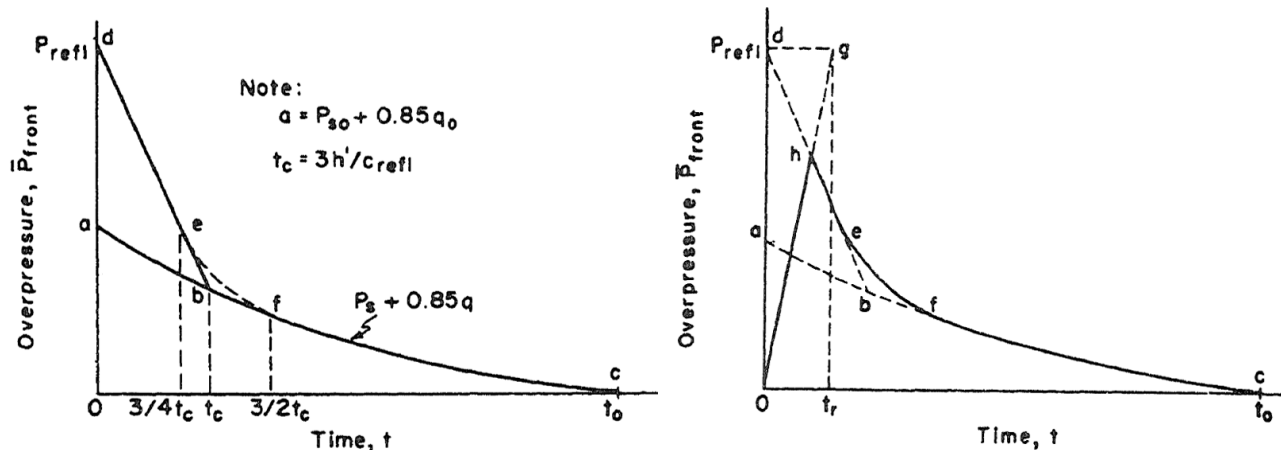


Figure 07:  $\bar{P}_{front}$  versus Time. Time to Rise  $t_r$  is Negligible



In **Figure 07** (right side), the time to rise  $t_r$  must be considered by first computing the average front face overpressure for a zero time of rise; i.e., curve **O-d-e-f-c**. Locate point **g** with time coordinate  $t_r$  and overpressure coordinate  $P_{refl}$  and then join point **O** and **g** with straight line intersecting **d-e-f** at **h**. The average front wall overpressure for time of rise  $t_r$  is given by curve **O-h-e-f-c**.

The overpressure on the front wall of a structure is not uniformly distributed. The maximum value occurs at the mid-point of the base and the minimum value occurs along the edges. Those portions of the front face nearest to the edges are cleared of the reflection effects in a shorter time than the remainder of the front face and the overpressure existing at those points is lower, following the clearing stage.

The net effect of this vertical and horizontal variation is negligible and of questionable value for design purposes. Hence, the front wall loading is assumed to be distributed uniformly over the front wall surface. For the same reasons, the rear wall loading given next is assumed to be uniformly distributed over the rear wall.

### **Average Back Wall Overpressure, $\bar{P}_{back}$**

For the rear wall, the time-displacement factor  $t_d$  is  $L/U_0$  (Equation **E.10**), where  $L$  is the length of the building in the direction of propagation of the shock and  $U_0$  is the shock front velocity. When the shock front crosses the rear edge of the structure, the foot of the shock spills down the back wall.

The overpressures on the back wall behind this diffracted wave are considerably less than those in the incident blast wave due to the vortex which develops at the top and travels down the wall. A period longer than that required for the travel of this diffracted shock to the bottom of the wall must pass before the back wall average overpressure reaches its peak value. The time required for this build-up to occur,  $t_b$ , is measured from the instant at which the shockwave reaches the back wall and is estimated by using Equation **E.11**:

$$t_b = 4h'/c_0 \quad \text{E.11}$$

$h'$  : Clearing height of the back wall, taken equal to either the full height of the back wall or half the width of the building, whichever is the smaller

$c_0$ : T Velocity of sound in undisturbed air, i.e., 1115 ft·s<sup>-1</sup>

The peak value of the average overpressure on the back wall after this build-up has been completed is estimated by using Equation **E.12**:



$$(\bar{P}_{back})_{max} = P_{sb}(1/2)[1 + (1 - \beta)e^{-\beta}] \quad \text{E.12}$$

$P_{sb}$ : Incident blast wave overpressure (Equation E.01) at the back wall at time  $(t - t_d) = t_b$

$(\bar{P}_{back})_{max}$ : Peak value of the average overpressure on the back wall which occurs at time  $t = t_d + t_b$

$\beta$ : Dimensionless ratio estimated by using Equation E.13:

$$\beta = 0.5P_{s0}/14.7 \quad \text{E.13}$$

where  $P_{s0}$  is assumed to not diminish in strength as the wave passes over the structure.

For times where  $t_d < t < t_d + t_b$ , the  $\bar{P}_{back}$  is estimated as follows (Equation E.14):

$$\bar{P}_{back} = \frac{(\bar{P}_{back})_{max}}{t_b} t \quad \text{E.14}$$

For times where  $t_d > t_d + t_b$ , the  $\bar{P}_{back}$  is estimated as follows given  $t_0$  as the duration of the positive phase (Equation E.15):

$$\frac{\bar{P}_{back}}{P_s} = \frac{(\bar{P}_{back})_{max}}{P_{sb}} + \left[ 1 - \frac{(\bar{P}_{back})_{max}}{P_{sb}} \right] \left[ \frac{t - (t_d + t_b)}{t_0 - t_b} \right]^2 \quad \text{E.15}$$

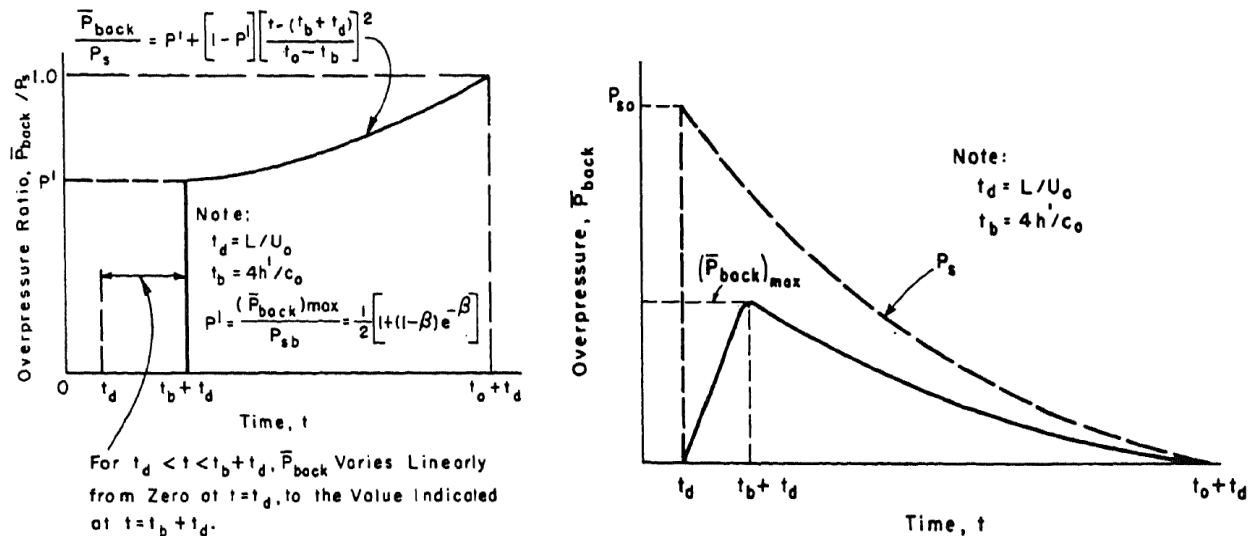


Figure 08:  $\bar{P}_{back}$  versus time



### Average Net Horizontal Overpressure, $\bar{P}_{net}$

Considering as positive all overpressures exerted on the structure and directed toward the interior, the average net horizontal overpressure is estimated as follows (Equation E.16):

$$\bar{P}_{net} = \bar{P}_{front} - \bar{P}_{back} \quad \text{E.16}$$

### Roof Overpressure, $\bar{P}_{roof}$

The procedure developed for prediction of overpressures on the roof of a structure is based primarily on curve-fitting of the Princeton and Michigan shock tube data [2], [12], [15], [16], [17], [18], [19] and [20]. Pressures calculated by this procedure have been found to agree satisfactorily with overpressure records obtained in the GREENHOUSE structure testing program and the Sandia HE tests [19].

During the passage of the blast wave across the structure, low pressure areas develop on the roof and side walls due to vortex formation. Shock tube data indicate that this vortex detaches itself from the front edges and moves across the structure with gradually increasing speed. Vortices are formed all along the front edges of the roof and sides of the structure; i.e., along **a-b-c-d** of Figure 10. At corners **b** and **c** where they are aligned at 90° to each other, the vortices tend to interfere with each other and to move away from the roof and wall surfaces. This results in a diminution of the effects of the vortices at these edges which proceeds along the axes of the vortices from corners **b** and **c** as the vortices move toward the rear of the roof. Consequently, the regions on the roof and side walls which are strongly affected by the vortices do not extend to all edges of the roof, but are triangular or trapezoidal in shape as indicated in Figure 09.

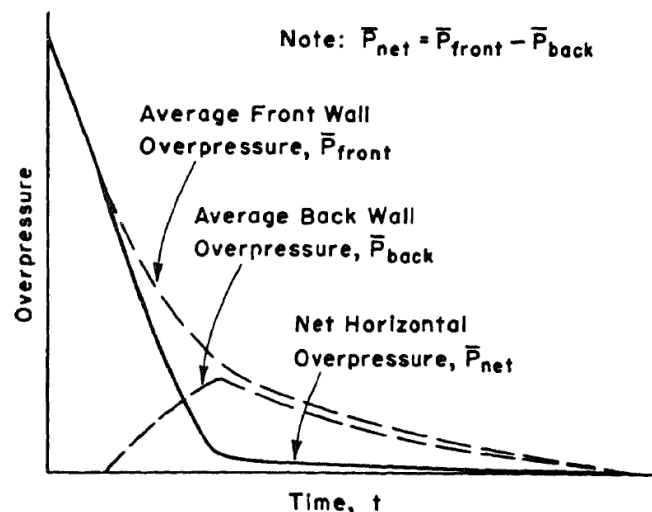
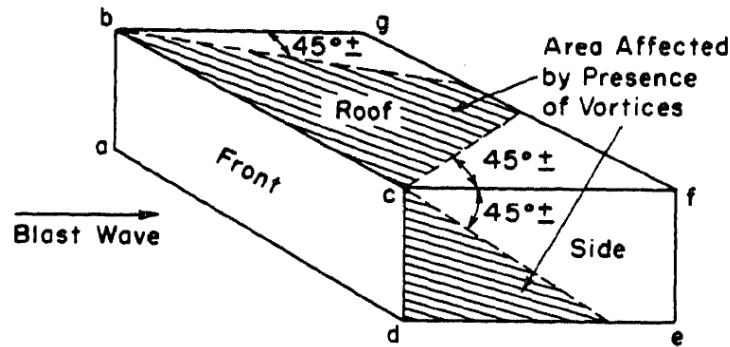
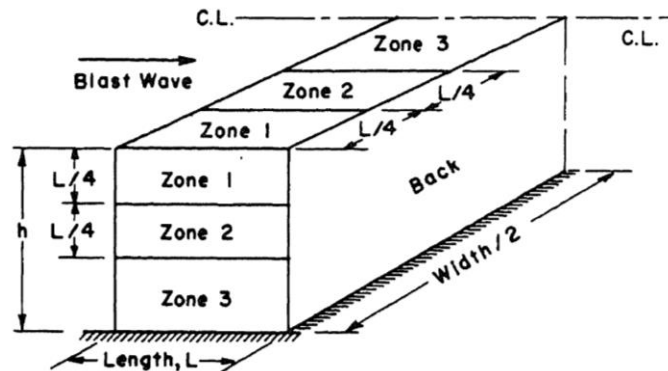


Figure 09: Net Horizontal Overpressure  $\bar{P}_{net}$  versus Time



**Figure 10: Areas on Roof and Sides Most Affected by Vortex Action**

These observed results indicate a variation of overpressures on the roof in a direction parallel to the shock front in addition to a variation along the roof in the direction of propagation of the wave. Although this lateral variation is a smooth one, the roof and side walls are divided into three (3) zones as illustrated in **Figure 11** to facilitate computation of local pressures. Although only the location of the zones on the roof is discussed below, the zones on the side wall are similarly located as shown in **Figure 11**.



**Figure 11: Location of Loading Zones on Roof and Sides of Structure**

**Zone 1 - Local Roof Overpressure,  $P_{roof}$**

This zone is a strip on the roof extending from the sides toward the center line a distance equal to one-quarter of the length  $L$  of the building. **Figure 12** is a plot of  $P_{roof}/P_s$ , the ratio of the local overpressure at any point on the roof in terms of time  $t$  to the overpressure in the incident blast wave where  $t_d = L'/U_0$  (Equation **E.10**) is the timed-displacement factor, equal to the time required for the shock front to travel a distance  $L'$ , the distance from the front edge of the roof to the point under consideration. **Figure 12** indicates that the local overpressure versus time curve for any point in Zone 1 is equal to the overpressure-time curve for the incident blast wave displaced in time by factor  $t_d = L'/U_0$ . This is consistent with observed vortex disintegration as illustrated in **Figure 11**.



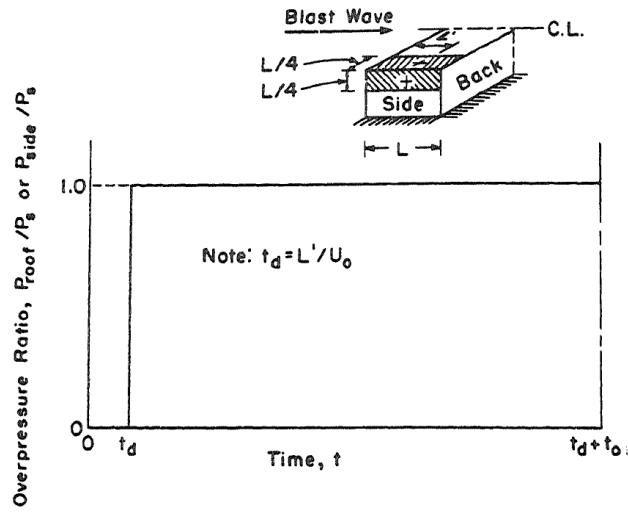


Figure 12: Local Roof or Side Wall Overpressure Ratio versus Time – Zone 1

**Zone 2 - Local Roof Overpressure,  $P_{roof}$**

This zone is a strip on the roof of width equal to one-quarter of the length of the structure measured from the edge of Zone 1 toward the center of the roof. **Figure 13** is a plot of the ratio  $P_{roof}/P_s$  for any point a distance  $L'$  from the front edge of the roof. Here again,  $P_{roof}$  and  $P_s$  incorporate the time-displacement  $t_d = L'/U_0$ .

\*Note that  $t_m$  is defined below when addressing Zone 3.

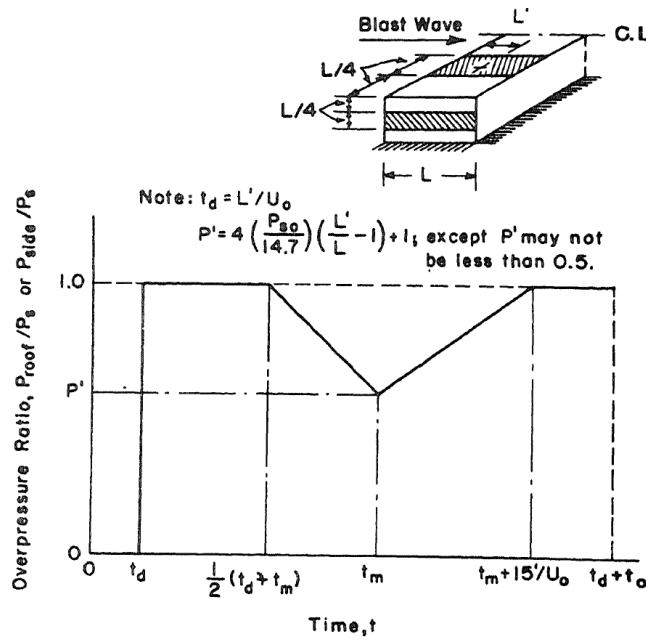
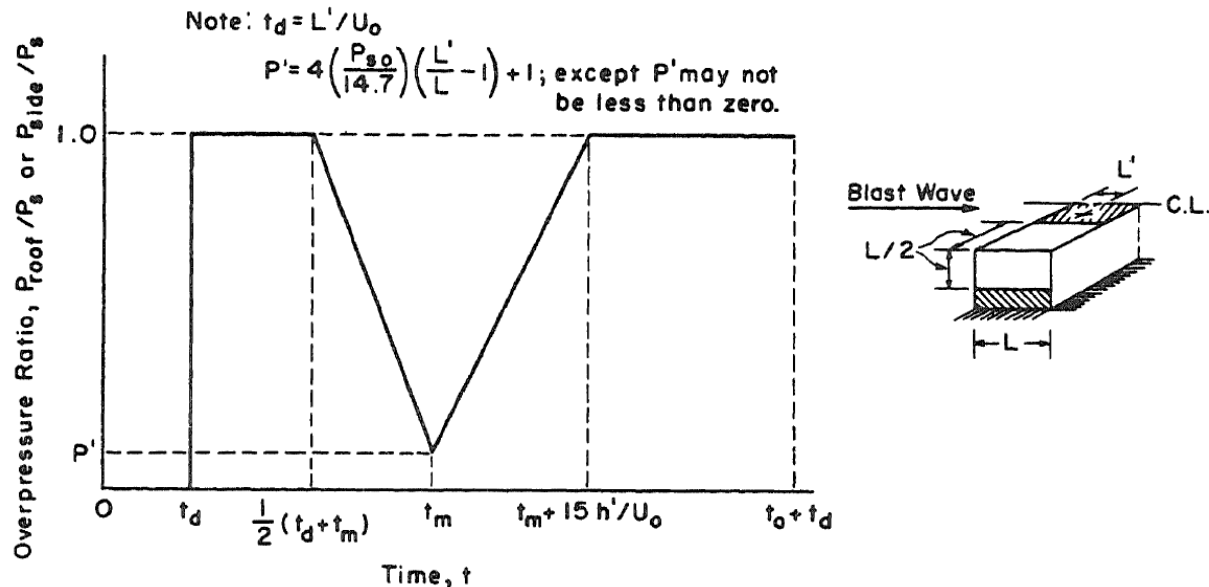


Figure 13: Local Roof or Side Wall Overpressure Ratio versus Time – Zone 2



### Zone 3 - Local Roof Overpressure, $P_{roof}$

This zone includes all points on the roof not included in Zones 1 and 2. **Figure 14** is a plot of the ratio  $P_{roof}/P_s$  for all points in this zone. Zone 3 is essentially a region of two-dimensional shock phenomena for which considerable data are available in [2], [12], [15], [16], [17], [18] and [19].



**Figure 14: Local Roof or Side Wall Overpressure Ratio versus Time – Zone 3**

The effects of the vortex travel across the roof of the structure are confined to Zones 2 and 3. The difference in the overpressure existing in these zones is due to the assumed severity of the vortex effects.

As the shock front passes over the point being considered, the local overpressure is raised to the overpressure in the incident blast wave. This equality between local and incident blast wave overpressures is maintained until the vortex developed at the front edge of the roof detaches itself and moves toward the rear edge, causing a decrease from the overpressure in the incident blast wave at the point being considered. The local overpressure reaches its minimum value at the time that the vortex is over the point in question. The time required for the vortex to travel the distance  $L'$  is  $t_m = L'/v$  (Equation E.17) where  $v$  is the vortex travel velocity, obtained from a reduction of the data in reference [4] and given by Equation E.18:

$$v = \left( 0.042 + 0.108 \frac{L'}{L} \right) U_0 \quad \text{E.18}$$

The following criteria is applicable for defining the roof overpressure history in both Zone 3 and Zone 2:



The value of the ratio  $P_{roof}/P_s$  at time  $t < t_d$  is:

$$P_{roof}/P_s = 0 \quad \text{E.19}$$

The value of the ratio  $P_{roof}/P_s$  at time  $t_d \leq t < (t_d + t_m)/2$  is:

$$P_{roof}/P_s = 1 \quad \text{E.20}$$

The value of the ratio  $P_{roof}/P_s$  at time  $(t_d + t_m)/2 \leq t < t_m$  is:

$$\frac{P_{roof}}{P_s} = \left[ \frac{2(1 - P')}{t_d + t_m} \right] t \quad \text{E.21}$$

The value of the ratio  $P_{roof}/P_s$  at time  $t = t_m$  is:

$$P' = \frac{P_{roof}}{P_s} = 4 \left( \frac{P_{so}}{14.7} \right) \left( \frac{L'}{L} - 1 \right) + 1.0 \quad \text{E.22}$$

- $P' \geq 0.5$  for points located in Zone 2
- $P' \geq 0$  for points located in Zone 3

As soon as the vortex has passed the point in question, the local overpressure starts to build up until at time  $t = t_m + 15h'/U_0$  (where  $h'$  is the clearing height of the structure) it is once again equal to the overpressure in the incident shockwave. The value of the ratio  $P_{roof}/P_s$  at time  $t_m \leq t < t_m + 15h'/U_0$  is:

$$\frac{P_{roof}}{P_s} = \left[ \frac{U_0(1 - P')}{15h'} \right] t \quad \text{E.23}$$

Finally, the value of the ratio  $P_{roof}/P_s$  at time  $(t_m + 15h'/U_0) \leq t < (t_d + t_0)$  is:

$$P_{roof}/P_s = 1 \quad \text{E.24}$$

### **Average Roof Overpressure versus Time**

Having established the variation of local overpressure, the average overpressure on the roof at any time,  $\bar{P}_{roof}$  could be obtained by the summation of the local overpressure curves over the entire roof at a given time  $t$ . If there were no lateral variation of local overpressures, such a method could be used to develop a general procedure applicable to all structures. However, the presence of this lateral variation complicates any procedure to such a degree that only the limiting case for Zone 3 loading is considered. The ratio  $\bar{P}_{roof}/P_s$  is plotted in **Figure 15** for times more than time  $t_d = L/U_0$  where  $P_s$  incorporates the time-displacement,  $t_d = L/2U_0$ .



The average overpressure on the roof varies linearly from zero at time  $t = 0$  to the value of  $\bar{P}_{roof}$  given in **Figure 15** at time  $t = L/U_0$ . The assumption that  $\bar{P}_{roof}$  can be expressed as a proportion of  $P_s$  is valid only if the time required for the shock front to travel the length of the building is small compared to the duration of the positive phase. For values of  $(L/U_0)/t_0$  less than 0.1 this assumption is reasonable.

A farther restriction must be imposed due to the importance of the lateral variation of overpressures on the roof. If the width of the structure normal to the direction of travel of the shock wave is greater than twice its length, the average roof overpressures as determined by **Figure 15** are satisfactory. For a structure whose width is less than its length, the average roof overpressure for times greater than time  $t = L/U_0$  is more correctly given by the relation  $\bar{P}_{roof} = P_s$ , where  $P_s$  incorporates the time-displacement  $t_d = L/2U_0$ . The average roof overpressure varies linearly from time  $t = 0$  to the value calculated by Equation  $\bar{P}_{roof} = P_s$  at time  $t = L/U_0$ . For structures which are approximately square in roof plan, an average of the two methods discussed should be used.

If a more accurate value of the average overpressure on a portion of the roof, such as a roof slab, is desired, this may be obtained by computing the local overpressure at two or three points on the slab and obtaining the weighted average as a function of their common time  $t$ .

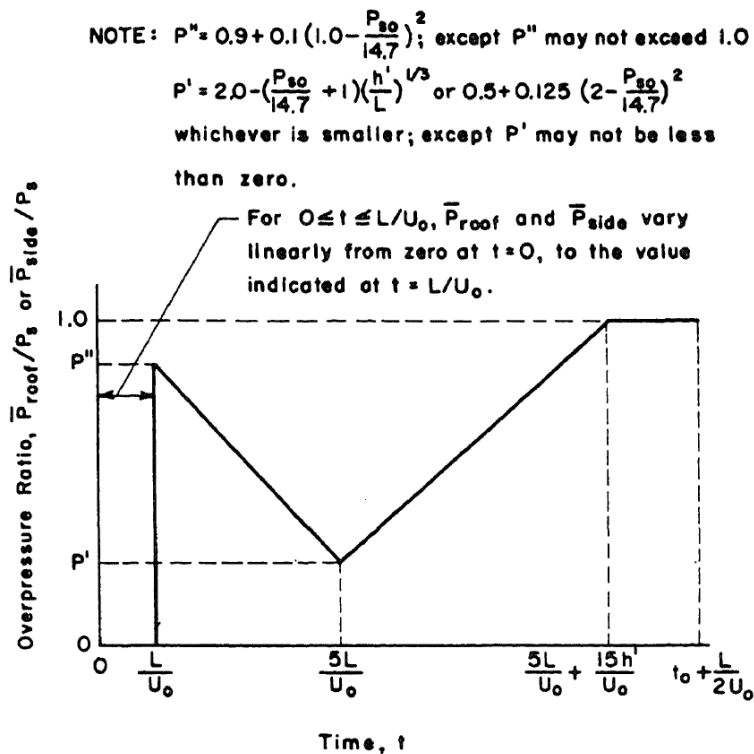


**Figure 15:**  $\bar{P}_{roof}$  or  $\bar{P}_{side}$  versus Time



The value of the ratio  $P_{roof}/P_s$  at time  $t_d = L/U_0$  is given by Equation E.25:

$$P'' = \frac{P_{roof}}{P_s} = 0.9 + 0.1 \left(1 - \frac{P_{so}}{14.7}\right)^2 \quad \text{E.25}$$

The value of the ratio  $P_{roof}/P_s$  at time  $t_d = 5L/U_0$  is given by Equation E.26:

$$P' = \frac{P_{roof}}{P_s} = \min \left\{ \left[ 2 - \left( \frac{P_{so}}{14.7} + 1 \right) \left( \frac{h'}{L} \right)^{\frac{1}{3}} \right], 0.5 + 0.125 \left( 2 - \frac{P_{so}}{14.7} \right)^2 \right\} \quad \text{E.26}$$

\*Note that  $(P'')_{max} = 1$  and  $(P')_{min} = 0$

The value of the ratio  $P_{roof}/P_s$  at time  $L/U_0 \leq t < 5L/U_0$  is given by Equation E.27:

$$\frac{P_{roof}}{P_s} = \left[ \frac{U_0(P'' - P')}{4L} \right] t \quad \text{E.27}$$

Finally, the value of the ratio  $P_{roof}/P_s$  at time  $5L/U_0 \leq t < 5L/U_0 + 15h'/U_0$  is given by Equation E.28:

$$\frac{P_{roof}}{P_s} = \left[ \frac{U_0(1 - P')}{15h'} \right] t \quad \text{E.28}$$

### **Average Side Overpressure, $\bar{P}_{side}$**

Based on test data, it has been observed that the sides of a structure are loaded in the same manner as is the roof and that **Figure 10 to Figure 15** determined for the roof of a structure apply equally well to the sides. The side walls are divided into three zones, as shown in **Figure 11** for the determination of local overpressures  $P_{side}$ . **Figure 12 to Figure 15** present these local overpressures in the form  $P_{side}/P_s$  where  $P_{side}$  and  $P_s$  incorporate the time-displacement  $t_d = L'/2U_0$  and  $L'$  is the distance from the front edge of the side wall to the point under consideration.

The average overpressure on the side is given as the ratio  $\bar{P}_{side}/P_s$  in **Figure 15** where  $P_s$  is the overpressure in the incident blast waves with a time-displacement  $t_d = L/2U_0$ . **Figure 15** is applicable only if the height  $h$  of the side wall is greater than half the length  $L$ . If this restriction is not satisfied the average overpressure on the side is more correctly given by the relation  $\bar{P}_{roof} = P_s$



## Conclusions

The major concerns for anyone involved with risk assessment related to explosions is to estimate the explosion wave shape and the overpressure and impulse as a function of distance from the explosion. Once these key parameters are known, the damage effects to people and structures/buildings can be estimated. Detailed damage criteria to humans due to explosions can be found in reference [13].

The blast loading on a structure is needed to evaluate the building/structure damage and to estimate the indoor injury or fatality rate. Blast loading requires the evaluation of the interaction between the blast wave and the impacted structure and its main purpose is to estimate pressure history profiles at each side/roof of the structure. This information is a critical step before conducting the Single Degree of Freedom (SDOF) approach once the resistance of the structure is known. The development of the SDOF approach can be found in reference [14].

As a summary, the present paper introduces the explosion basics and is focused on blast loading phenomena to structures. This is a key parameter for calculating the structural response by using the Single Degree of Freedom (SDOF) approach.



## References

- [1] Crowl, D.A., 2003. "Understanding Explosions". A CCPS Concept Book. Center for Chemical Process Safety of the American Institute of Chemical Engineers. New York, New York.
- [2] Baker, W. E., Cox, P. A., et al., 1988. "Explosion Hazards and Evaluation". Elsevier Scientific Publishing Co., New York.
- [3] AIChE, 1994. "Guidelines for Evaluating the Characteristics of Vapor Cloud Explosions, Flash Fires and BLEVEs". American Institute of Chemical Engineers. New York, New York.
- [4] AIChE, 1999. "Guidelines for Consequence Analysis of Chemical Releases". American Institute of Chemical Engineers. New York, New York.
- [5] Brode, H. L., 1959. "Blast Waves from a Spherical Charge" *Phys. Fluids*, 2: 217.
- [6] Melhem, G. A., 2016. "Advanced Consequence Analysis: Fluid Flow, Emergency Relief System Design, Thermal Hazards Assessment, Emission, Dispersion, Fire and Explosion Dynamics". ioMosaic Corporation.
- [7] Lees, F. P., 1996. "Loss Prevention in the Process Industries". Second Edition. Butterworth Heinemann, Oxford.
- [8] AIChE, 2000. "Guidelines for Chemical Process Quantitative Risk Analysis". Second Edition. American Institute of Chemical Engineers. New York, New York.
- [9] Benuzzi, A., Zaldivar, J. M., 1991. "Safety of Chemical Batch Reactors and Storage Tanks", Kluwer Academic Publishers, Dordrecht, The Netherlands.
- [10] AIChE, 1995. "International Symposium on Runaway Reactions and Pressure Relief Design". American Institute of Chemical Engineers. New York, New York.
- [11] Eckhoff, R. K., 2003. "Dust Explosions in the Process Industries". Third Edition. Gulf Professional Publishing.
- [12] Army Technical Manual TM 5-1300 and UFC 3-340-02., 1990. "Structures to Resist the Effects of Accidental Explosions". Departments of the Army, the Navy and the Air Force.
- [13] Dunj3, J., Amor3s, M., Prophet, N., Gorski, G., 2016. "An Overview of State-of-the-Art Damage Criteria for People and Structures". An ioMosaic White Paper, ioMosaic Corporation.



**[14]** Dunj6, J., Amor6s, M., Prophet, N., Gorski, G., 2016. "Risk-Based Approach – Explosions and Structural Response. Introduction to Single Degree of Freedom and Pressure-Impulse Diagram". An ioMosaic White Paper, ioMosaic Corporation.

**[15]** US Army Corps of Engineers. "Design of Structures to Resist the Effects of Atomic Weapons". Manuals:

- EM 1110-345-413: Weapons Effects Data
- EM 1110-345-414: Strength of Materials and Structural Elements
- EM 1110-345-415: Principles of Dynamic Analysis and Design
- EM 1110-345-416: Structural Elements Subjected to Dynamic Loads
- EM 1110-345-417: Single-Story Frame Buildings

**[16]** Biggs, J. M., 1964. "Introduction to Structural Dynamics". McGraw-Hill, ISBN: 07-005255-7.

**[17]** US Army Corps of Engineers, 2008. "Methodology Manual for the Single-Degree-Of-Freedom Blast Effects Design Spreadsheets (SBEDS)". PDC TR-06-01.

**[18]** ASCE, 2008. "Design of Blast Resistant Buildings for Petrochemical Facilities". Second Edition. American Society of Civil Engineers (ASCE).

**[19]** Cormie, D., Mays, G., Smith, P., 2009. "Blast Effects on Buildings". Second Edition. ICE Publishing, 40 Marsh Wall, London E14 9TP.

**[20]** AISC, 2005. "Steel Construction Manual". Thirteenth Edition. American Institute of Steel Construction (AISC). ISBN: 1-56424-055-X.